Assessment of the hydrological impacts of green roof: From building scale to basin scale

P.-A. Versini, D Ramier, E Berthier, B De Gouvello

Assessment of the hydrological impacts of green roof: from building scale to basin scale

P.-A. Versini [1,*], D. Ramier[2], E. Berthier[2], B. de Gouvello[1]

1 Centre Scientifique et Technique du Bâtiment (CSTB) et Laboratoire Eau Environnement et Systèmes Urbains (LEESU-ENPC), 6-8 avenue Blaise Pascal 77455 Marne-la-Vallée, France

2 CEREMA, Direction territoriale d'Île-de-France, , 12 rue Teisserenc de Bort, 78190 Trappes-en-Yvelines, France

* Corresponding author: pierre-antoine.versini@leesu.enpc.fr, LEESU-ENPC, 6-8 avenue Blaise Pascal 77455 Marne-la-Vallée, France, Tel= +33 164 15 37 54, Fax : +33 165 64 15 37 64.

Abstract:

At the building scale, the use of green roof has shown a positive impact on urban runoff (decrease and slow-down in peak discharge, decrease in runoff volume). The present work aims to study whether similar effects are possible at the basin scale and what is the minimum spreading of green runoff needed to observe significant impacts. It is particularly focused on the circumstances of such impacts and how they can contribute to storm water management in urban environment. Based on observations on experimental green roofs, a conceptual model has been developed and integrated into the SWMM urban rainfall-runoff model to reproduce the hydrological behaviour of two different types of green roof. It has been combined with a method defining green roofing scenarios by estimating the maximum roof area that can be covered.

This methodology has been applied on a long time series (18 years) to the Châtillon urban basin (Haut-de-Seine county, France) frequently affected by urban flooding. For comparison, the same methodology has been applied at the building scale and a complementary analysis has been conducted to study which hydrometeorological variables may affect the magnitude of these hydrological impacts at both scales.

The results show green roofs, when they are widely implemented, can affect urban runoff in terms of peak discharge and volume, and avoid flooding in several cases. Both precipitation – generally accumulated during the whole event- and the initial substrate saturation are likely to have an impact on green roof effects. In this context, the studied green roofs seem useful to mitigate the effects of usual rainfall events but turn out being less helpful for the more severe ones. We conclude that, combined with other infrastructures, green roofs represent an interesting contribution to urban water management in the future.

Keywords: Green roof, hydrological modelling, SWMM, flooding, sewage network

1-Introduction

Historically used for isolation purposes in Nordic countries, green roofs have become relatively commonplace over the last 20 years in countries subject to more continental climate as Germany, Austria and Switzerland. In the last years, the spread of green roofs has steadily increased in developed countries. The annual green roof covering is estimated between 0.1 and 1 km^2 in several countries all over the word (Spain, Brazil, Canada, Korea, UK or Japan), while it is estimated to reach 2 km^2 in France and even more than 10 km^2 in Germany (Lassalle, 2012).

Such a success is part of the general policy of urban areas revegetation and can be explained by two main reasons. First, roof areas represent a significant part of the surfaces of city centres where no space is available for new infrastructures (about 40-50% of the impervious areas, cf. Dunnett and Kingsbury, 2004). Secondly, from an architectural point of view, green roofs may contribute to enhance the aesthetic value of buildings, but also to reduce heat island through increasing evapotranspiration (Takebayashi and Moriyama, 2007; Santamouris, 2012), to improve the quality of the air (Banting *et al.*, 2005), to protect biodiversity (English Nature, 2003) and to manage urban runoff.

This last point - urban runoff management – is a significant argument to promote the development of green roof. Indeed, in order to cope with urbanization and its related problem of space, green roofs –as well as porous pavements, harvesting tanks, soakaways or ponds- are part of the so called stormwater Source Control (SC) which has gained relevance over traditional sewer approaches (Urbonas and Jones, 2002; Delleur, 2003; Petrucci *et al.*, 2012). The principle of SC is to develop, simultaneously to urban growth, facilities to manage stormwater at a small-scale (about 10^2–10^3 m^2) to solve or prevent intermediate scale (10^4–10^6 m^2) stormwater issues. At the building scale, green roofs have the possibility to control both the quantity and the quality of urban runoff. Qualitatively, it can avoid the direct contribution of metals to receiving water as traditional roofs (Egodawatta *et al*., 2009; Gromaire *et al*., 2011). Nevertheless, an increase in phosphorous concentration due to vegetation coverage can be noticed (Gromair*e et al*., 2013). From a quantitative point of view, the main performance of green roofs in stormwater management is the reduction of runoff volume at the annual scale and the peak attenuation and delay at the rainfall event, depending essentially on the green roof configuration, the rainfall intensity and the antecedent soil moisture conditions.

These quantitative impacts have already been studied by several works based on observation or modelling. Typically, quite small surfaces of experimental green roofs were instrumented to set continuous runoff and precipitation data on short periods of time (not exceeding 3 years). These data are then analysed to study and explain the fluctuation of green roofs responses in terms of peak discharge and runoff volumes.

A very small test bed of 3 m^2 comprising sedum extensive vegetation growing in 80 mm of substrate was conducted by Stovin *et al.* (2012) in Sheffield (UK). The rainfall-runoff monitoring was performed continuously over a period of 29 months. The annual cumulative retention was 50% and the peak attenuation ranged from 20 to 100% (median of 59%). In this case, it was not possible to establish any relationship between rainfall retention percentage and the storm characteristics or the antecedent weather variables.

Voyde *et al.* (2010) instrumented six hydraulically isolated plots of about 10-50 m^2 on the Aukland University (New Zealand) during one year. These plots differed according to their substrate types (expanded clay, zeolite and pumice) and depths (50 or 70 mm). Except for one specific plot where coconut coir fibre was implemented in the sedum mat, there was no statistically significant difference in the hydrologic response from the three different substrate types. During the year-long experiment, 66% of precipitation was retained and a peak flow reduction ranging from 31% to 100% (median of 93%) was observed. Moreover, no statistically significant season-related variations were also recorded for either rainfall or runoff response. On the same site, additional data (2 years) were analysed by Fassman-Beck *et al*. (2013) and similar results in terms of water balance were obtained. Nevertheless, statistically significant seasonal variation was observed, demonstrating the importance of long-term monitoring.

A larger surface was covered by green roof in Genoa (Italy) where about 350 m^2 were divided in two plots, each one comprising a substrate of 200 mm and drainage layer (Palla *et al.*, 2011) differentiated according to their substrate mix. At the event scale, the study, carried out over 6 months, showed a retained volume varying between 10 and 100% (average of 85%), and a peak flow reduction ranging from 80 to 100% (average of 97%).

Additional studies can be mentioned: Monterusso *et al*., 2004 ; Bengtsson *et al*., 2005 ; Dunnett *et al*., 2008 ; Gregoire and Clausen, 2011 among others. They all conclude, and sometimes contradictorily, that green roof response appears not to be link to one only factor. These numerous contributions show several parameters may have an impact on hydrological response such as rainfall accumulation and intensity (Carter and Rasmussen, 2006 ; Simmons *et al*., 2008), the climatic conditions, seasonality (Mentens *et al*., 2006 ; Villarreal, 2007), the antecedent conditions (Bengtsson *et al*., 2005 ; Denardo *et al*., 2005), and to a lesser extent, the substrate species and the depth or roof slope (Villarreal and Bengtsson, 2005 ; Getter *et al*., 2007). A detailed review on the influence of these parameters is available in Berndtsson (2010). It has also to be noticed that recent studies conducted over a longer time period (Carson *et al*., 2013; Fassman-Beck *et al*., 2013) show that rainfall depth appears to be the dominant factor in retention performance.

On the other side, few works attempted to simulate the hydrological response of green roof by using adapted models. They were usually devoted to reproduce observed runoff at the experimented roof scale or to extrapolate the green roof impact at the urban catchment scale. Hilten *et al.* (2008) tested HYDRUS-1D (Šimůnek *et al*., 2008) which is a soil moisture transport simulation using Richards' equation for variably-saturated water and convection-dispersion type equations. They tried to simulate the hydrological response of a 37 m^2 green roof. Although HYDRUS-1D was able to correctly reproduce runoff for small rain events, it failed for the largest ones by overestimating the peak discharge.

The SWMS_2D model (Šimůnek *et al*., 1994), based on Richards' law and the Van Genuchten–Mualem functions, was also applied to simulate the variably saturated flow of an experimental green roof system (Palla *et al*., 2009). Applied on 8 rainfall events, the model adequately reproduced the hydrographs, as demonstrated by the limited relative percentage deviations obtained for the total discharged volume, the peak flow, the hydrograph centroid and the water content along the vertical profile.

Simplified procedures were used to model green roof at a greater scale than the building one. Palla (2008a) used the Soil Conservative Service (SCS) Curve Number (CN, Mockus, 1957) as infiltration model in an aquifer system to simulate green roof response at the catchment scale in the Storm Water Management Model (SWMM, Rossman, 2004). It was calibrated using results from a small size system realized in laboratory then applied on a 18 years simulation period. It was also the case in Carter and Jackson (2007) where the SCS infiltration method was used to simulate green roof response with a CN value equal to 86. Using synthetic precipitation events they evaluated the impact of a widespread green roof application in an urban watershed.

Additionally, some efforts were made to build a simple and robust model of green roof hydrological behaviour, in order to be used as a support tool devoted to extensive green roof design (Berthier *et al*., 2011). Based on a reservoir cascade, this model appeared suitable to reproduce the hydrological behaviour of a 146 m^2 green roof located in Paris region (France) during one year.

Although the literature on green roof hydrological impacts has greatly developed in the last years, still few works have concentrated on to study long time period and on their use to solve urban management issues. Using a modelling system developed from an experimental setup, the work presented herein aims to study the green roof impacts on urban runoff over 18 years comprising a large and heterogeneous set of hydrometeorological situations. By comparing the results obtained at the building scale and at the basin scale, this paper is particularly focused on: (1) how far the dissemination of green roofs at large scale may affect urban runoff as much as for the building scale, (2) what are the main factors conducting the hydrological response at both scales and to what extent are they predictable.

The paper is structured as follows: Section 2 presents the specific model developed to estimate green roof hydrological response. Section 3 describes the studied basin, the geographical and meteorological data used. Section 4 presents the modelling framework and the methodology used in this study. Assessment of hydrological impacts of a green roof at the roof scale and at the basin scale is presented in Section 5. From a more operational point of view, Section 6 analyses the conditions of these hydrological impacts on stormwater management and how they can be predicted by taking into account several hydrometeotrological variables. Finally, Section 7 discusses the hypothesis made in the study and Section 8 summarizes the main results and concludes on future improvements and possible applications of green roofs for operational issues.

2- Green roof modelling

2-1 Experimental setup

An experimental green roof was built on the site of the CEREMA in Trappes (45 km South-West from Paris, France). The area of an already existing roof was split into 6 different plots of 35 m^2 (7X5 m). These plots were covered by a specific green roof infrastructure presenting different configuration in terms of vegetation (sedum or grass), substrate depth (3 or 15 cm) and drainage layer (expanded polystyrene or lava stone). Rainfall and discharge were continuously monitored at each plot from June 2011 to August 2012. Rainfall was measured with a tipping bucket raingauge located on the roof, with a resolution of 0.1 mm. Discharge from each plot was measured continuously at the outlet of the downspouts with custom-made PVC tipping bucket, having a resolution of 0.01 mm (i.e. a volume of 350 ml per tip over the 35m^2 plot). Time series were aggregated to 3 minutes intervals.

In this study, observations from two specific configurations of green roof were used. They combine an extensive vegetation layer made with a mix of Sedum species (S. Album, S. Sexagulare, S. Reflexum, S. Kamchatikum, S. Spurium, S. Acre), a substrate with lapillus, peat and green compost (organic part represents 3.4% in mass of the substrate), a filter layer (geotextile) and a drainage layer with expanded polystyrene of

4 cm depth. The two green roof configurations differ in terms of the depth of the substrate. For the first one, called SE3Y, the thickness is 3 cm and for the second one, called SE15Y, the thickness is 15 cm.

During the study time period, around 100 rain events (for a total rainfall of 827 mm) were observed for which rainfall accumulation was higher than 1 mm. They were all quite “soft” events and characterized by low return periods (the highest is about 1 year). These events produced runoff in most cases for green roof SE3Y plot (59% of the events) and less often for SE15Y one (45% respectively). It appeared the volumetric runoff coefficient for both green roof configurations varied significantly from an event to another, ranging from 0 to 1 with an average value of 0.17 for SE3Y and from 0 to 0.82 with an average value of 0.11 for SE15Y respectively. As mentioned in a previous study (Voyde *et al.*, 2010), retention efficiency seems to decrease as storm depth increases and as antecedent conditions reveal a high level of moisture in the substrate. For the most significant events, volumetric runoff coefficients are quite equal between both configurations and can occasionally be higher for SE15Y configuration if the substrate already contained water resulting from a previous event. Due to the short number of events, for now no definitive conclusion can be stated.

Note that more details on the experimental site is available in Gromaire *et al.* (2013). In this study, this data are only used to develop and calibrate the hydrological model.

2-2 Presentation of the hydrological model

Storm Water Management Model (SWMM version 5.0, see Rossman, 2004) has been used in this study. It is a dynamic rainfall-runoff model especially developed by the United States Environmental Protection Agency (EPA) for urban/suburban areas. The sewer network including junction nodes, conduits, and specific infrastructures (weir, orifice, storage unit …), is designed to simulate and estimate the hydrological behaviour of a typical basin. As SWMM is a semi-distributed model, each basin is divided in several sub-basins on which the water balance is computed. The SWMM module called "Bio-retention Cell" has been used and significantly modified to simulate the hydrological response of the instrumented green roofs as this original module was not able to do it accurately. Modifications are inspired by the model developed by Berthier *et al.* (2011) representing each layer of green roof infrastructure (vegetation, substrate and drainage) by 3 different reservoirs (Figure 1). The main modifications concern the vegetation reservoir (that produces discharge only when the field capacity is reached), the soil reservoir (by using the saturated hydraulic conductivity to produce discharge and by splitting its output into two components), and a transfer function that has been added to every reservoir output. This model is presented in detail in the following sections (note that simulated discharges, precipitation, simulated evapotranspiration and simulated reservoir levels are all expressed as water levels (mm) over the 35 m^2 plot).

A first reservoir models the vegetation layer which is supposed to retain a small amount of rainfall. If the storage capacity of the vegetation layer is lower than the precipitation, the complementary part of the precipitation (*Q_veg (t)*) infiltrates into the substrate:

$$Q\_veg(t) = \max\left[P(t) - \left(H\_veg - N\_veg(t)\right), 0\right] \qquad \text{(Eq. 1)}$$

Where *H_veg* is the vegetation reservoir depth (i.e. the maximum water depth stored by the vegetation layer), *N_veg(t)* is the vegetation reservoir level a time t, and *P(t)* is the precipitation rate.

The second reservoir represents the substrate layer which can produce surface runoff when it is saturated (*Q_sat (t)*) when it is no longer able to infiltrate water (it has to be noticed that this rare situation was not observed on Trappes experimental sites, even for the thinnest substrate):

$$Q\_sat(t) = \max[Q\_veg(t) - (f\_sub - \theta(t)) \times H\_sub, 0] \qquad \text{(Eq. 2)}$$

Where *f_sub* is the substrate porosity, representing the soil fraction where water can be stored, $\theta(t)$ is the volumetric water content at time t, and *H_sub* the substrate depth. $N\_sub(t)=H\_sub \times \theta(t)$ represents the substrate reservoir water level at time t.

The substrate reservoir produces an output discharge (*Q_sub (t)*) when the water content in the substrate is greater than the field capacity:

$$Q\_sub(t) = \max[\frac{Ksat}{\Delta t \times H\_sub} \times (\theta(t) \times H\_sub - FC), 0] \qquad \text{(Eq. 3)}$$

Where *Ksat* is saturated hydraulic conductivity (in mm/s), Δt is the time step (in s) and *FC* is the field capacity (in mm).

A small fraction *Q_frac(t)* of the output discharge is transferred to a routing reservoir representing the water temporary stored in the drainage layer:

$$Q\_frac(t) = Q\_sub(t) \times \left[1 - (1 - f\_dra) \times \left(\frac{N\_dra(t)}{H\_dra}\right)^4\right] \qquad \text{(Eq. 4)}$$

Where *f_dra* is the void fraction of the drainage layer, *N_dra(t)* is the routing reservoir water level, and *H_dra* is the routing reservoir depth.

At the output of the substrate, a runoff *Q_dra1(t)* is directly available while the routing reservoir produces a runoff *Q_dra2(t)*:

$$Q\_dra1(t) = Qsub(t) - Qfrac(t) \quad \text{(Eq. 5)}$$

$$Q\_dra2(t) = N_{dra}(t) + Qfrac(t) - H_{dra} \quad \text{(Eq. 6)}$$

Every contribution to the total discharge (*Q_sat(t), Q_dra1(t)* and *Q_dra2(t)*) are first routed to the outlet using a transfer function based on Manning-Strickler equation before being summed to *Q_tot(t)*:

$$Q\_rout(t) = \alpha \times Q*(t)^{\frac{5}{3}} \times \frac{L}{S} \quad \text{(Eq. 7)}$$

$$\alpha = \frac{1.49}{R} \times \sqrt{p} \quad \text{(Eq. 8)}$$

Where *Q_rout(t)* is the routed discharge assessed from *Q*(t)* (*Q*(t)* represents indiscriminately *Q_sat(t)*, *Q_dra1(t)* and *Q_dra2(t)*), S and L are the width and the area of the considered surface, R is the Manning roughness coefficient and p is the slope.

Evapotranspiration (ET) is estimated for each layer by using potential evapotranspiration computed by the French Weather service (PET daily measures in Villacoublay which is located 10 km from Trappes). The PET value is representative of the evapotranspiration for a short and always irrigated grass. To be more realistic, this data has been corrected by using seasonnal water balances computed with experimental data. PET data has also been adjusted by using a coefficient: 0.7 in winter and 0.9 in summer for SE3Y, 0.5 and 0.7 for SE15Y respectively. During dry periods (it is assumed that no evapotranspiration occurs during rain periods), water is evapotranspired from the top to the bottom, starting with the vegetation reservoir:

$$Eta\_veg(t) = Min\left(ET(t), N\_veg(t)\right) \quad \text{(Eq. 9)}$$

$$Eta\_sub(t) = Min\Big(Max\big(ET(t) - Eta\_veg(t), 0.\big), \big(H\_sub - WP\big) \times f\_sub\Big) \text{ (Eq. 10)}$$

$$Eta\_dra(t) = Min\Big(Max\big(ET(t) - Eta\_sub(t), 0.\big), N\_dra(t) \times f\_dra\Big) \text{ (Eq. 11)}$$

Where *ET(t)* is the estimated adjusted evapotranspiration, *WP* the wilting point, *Eta_veg(t)*, *Eta_sub(t)* and *Eta_dra(t)* the respective simulated evapotranspiration for vegetation, substrate and drainage layers.

At the end of each time step, reservoirs are updated by taking into account the different inputs and outputs. A Modified Puls method is used for this purpose as proposed in the initial version of SWMM.

The majority of the parameters characterizing the three green roof layers are determined by their intrinsic properties (geometry of the structure, thickness of the substrate and the layer of drainage, slope...). Finally, only four parameters have to be calibrated, essentially according the to substrate properties: porosity (*f_sub*), field capacity (*FC*), saturated hydraulic conductivity (*Ksat*) and roughness (*R*).

2-3 calibration and validation procedures

Observed precipitation and discharge data compiled from June 2011 to August 2012 in Trappes have been used to adjust the model parameters for SE3Y and SE15Y configurations. This observation period was divided into two sub-periods: from June 2011 to January 2012 for calibration and from February 2012 to August 2012 for validation. Both sub-periods contain a dry and a wet sequence. Wet sequences occurred in December 2011 (136 mm of the 472 mm have fallen during the calibration period) and in June 2012 (132 mm of the 345 mm have fallen during the validation period).

The model was calibrated by using a Rosenbrock procedure. Nash efficiency (Nash and Sutcliffe, 1970) was selected and used as the optimization criterion to evaluate the performance of the model (difference between observed and simulated discharges). It was computed for non-zero values to focus the calibration on wet sequences:

$$Nash = 1 - \frac{\sum_{i=0}^{n-1}\left(Qobs(t_0 + i\times\Delta t) - Qsim(t_0 + i\times\Delta t)\right)^2}{\sum_{i=0}^{n-1}\left(Qobs(t_0 + i\times\Delta t) - \overline{Qobs}\right)^2} \qquad \text{(Eq. 12)}$$

Where t_0 is the initial time step, $Qobs(t_0+i\times\Delta t)$ and $Qsim(t_0+ i\times\Delta t)$ are the observed and the simulated discharge at time step $t_0+ i\times\Delta t$, $\overline{Qobs}$ the average observed value and n the total number of time steps. Note that Nash criterion can be computed over a long time period or over a single event.

An additional indicator, the difference between observed and simulated total runoff volumes (absolute volume error), has also been computed:

$$V\_error = \frac{(Vobs - Vsim)}{Vobs}\times 100 \qquad \text{(Eq. 13)}$$

Where *Vobs* and *Vsim* are the observed and simulated total runoff volumes.

Satisfactory results were obtained for both green roof configurations for both calibration/validation continuous time periods. Almost every observed peak discharge was simulated and the highest peaks were particularly well represented. Nash efficiencies computed over the calibration period were higher than 0.7 (0.72 for SE3Y and 0.82 for SE15Y). This difference can be explained by the modest reproduction of SE3Y small peaks that are not generated by the SE15Y configuration. Moreover, volume errors showed that the water balance was correctly respected with some values lower than 10% (9% for SE3Y and 5% for SE15Y). These figures were slightly lower on the validation period (Nash equal to 0.64 for SE3Y and 0.80 for SE15Y and volume error equal to 5% for SE3Y and 9% for SE15Y). This seemed to be related to an overestimation of evapotranspiration. In this case, runoff volume was underestimated and some small peaks were not reproduced by the model. As the estimated daily evapotranspiration values were not realistic, it is a weakness of the model which influenced the draining of the reservoir during periods without rain.

An additional validation procedure was also carried out at the rainfall event scale. The average individual Nash efficiency and volumetric criteria were computed for every event for which the observed precipitation exceeded 8 mm (14 events). Average individual Nash value was 0.56 for SE3Y (volume error equal to 17%) and 0.55 for SE15Y respectively (volume error equal to 11%). It has to be noticed that the best results were usually obtained for the most important events of the time period. The comparison between observed and simulated discharges for the four main events is plotted in Figure 2 (Note that the first event belongs to the calibration period, whereas the other ones belong to the validation period). It appears that dynamics of runoff were well reproduced by the model. For these events, individual Nash efficiency was higher than 0.8 for SE15Y configuration and quite lower for the SE3Y one because of a delay of few minutes in the simulated response. For both configurations, the peak intensity was particularly well simulated with an absolute error lower than 10% in most of the cases.

Calibrated parameters are reported in Table 1. As the model structure is based on a simplification of the physical phenomena, the calibrated parameters were not always close to the range of values that might be expected from physical principles alone. Sometimes quite different values were calibrated for the same type of green roof."

Although they should be equal for both types of green roof configurations, Roughness (*R*=0.51 for SE3Y and *R*=0.65 for SE15Y) and saturated hydraulic conductivity (*Ksat*=104.7 mm/h for SE3Y and *Ksat*=2.0 mm/h) are different. While the SE3Y conductivity value is physically reasonable, the SE15Y one is very low, indicating the model's difficulty in representing the measured hydrological behavior with a simplified structure. This low value seems to be compensated by a lower Field Capacity (0.39 for SE3Y and 0.21 for SE15Y) or/and estimated evapotranspiration. As porosity (f_sub) is only used in the Q_sat computation, it has not been possible to calibrate it on the study time period (no surface runoff was observed or/and simulated). The theoretical value of 0.4 has also been used.

The aim of this simple model was to obtain an accurate and robust representation of green roofs' behaviour rather than an accurate representation of physics and parameters. Finally, despite small inconsistencies not affecting the representation of the main peak discharges, the results illustrate the ability of this new SWMM module to simulate green roof behaviour for both green roof configurations; particularly for the most important runoff that is the main point of interest in this study. Therefore, this model is used for this work to simulate the hydrological response of every building that could be covered by green roof at the basin scale. We also assume buildings' roofs are subject to the same conditions than Trappes ones in terms of geometric constraints (slope) and climate (French oceanic degraded climate).

3-Case study: the Hauts-de-Seine county

3-1 Case study framework

The Hauts-de-Seine county is located west of Paris (France). It is a highly populated and urbanized area (1.5 million inhabitants for a surface of 176 km^2). The northern part is very urbanised and limited by the Seine River, whereas the southern part is less populated with the presence of several forests. The climate of the Hauts-de-Seine is very close to the rest of Paris Basin (including Trappes) with mild winters, frequent rainfall in autumn, mild spring and high summer temperatures with possible occurrence of intense rainfall. The average annual rainfall over the county is about 700 mm, and rather constant over the different months, whereas the decennial hourly rainfall is about 35 mm.

Because of the rapid urbanization growth during the 90's and the difficulty to build new management infrastructures due to high density, stormwater network is very sensitive to intense precipitation which may cause local floodings. Since the beginning of 2000's, the local authority in charge of water management (Water Direction of the Haut-de-Seine county) has promoted mitigation solutions as Sustainable Urban Drainage System (SUDS). In this context, the Hauts-de-Seine county has set up a grant policy to promote regulated flat roofs and is also concerned with studying the impacts of existing and future green roofs on urban runoff in order to refine their approach in urban hydrology. Moreover, the implementation of green roofs is particularly interesting in this county because of the high development rate expected in this area over the next years.

Châtillon basin, chosen as case study, is located southeast of the Hauts-de-Seine county. It is a moderate urban basin of 2.37 km^2 characterized by a quite steep topography with an average slope of 3.5%. The dowstream part of the basin is essentially covered by individual housing, whereas the upstream part is rather covered by collective housing and economical activities (See Figure 3-a). Due to this intense urbanization, the basin is also characterized by an average impervious coefficient of 55%. Châtillon basin is equipped with combined sewer network supplied by waste water produced by 29,500 equivalent inhabitants. Local floodings often occur along the Boulevard de Vanves (see Figure 3), a main road crossing the city center. The pipe along the Boulevard until the outlet is not large or/and steep enough to route the runoff during intense rainfall. Note that there is a weir downstream of the Boulevard de Vanves and the basin outlet receives water that passes over this weir. Only the water exceeding the weir level is routed to the basin outlet. According to Water Direction of Hauts-de-Seine county, flooding occurs when the discharge exceeds the limit value of 4.7 m^3/s at the outlet (called "flooding threshold" in the following).

3-2 Hydrometeorological data

Regarding the meteorological information, the Hauts-de-Seine county is well covered by a rather dense raingauge network. A continuous precipitation database from a rain gauge located close to the Châtillon basin has been provided by the Water Direction of the county. It covers a full time period from 1993 to 2011 with a time resolution of 5 minutes. Note that, on this time period, the mean annual rainfall was 651 mm (snow is not considered) for a minimum of 435 mm in 2003 and a maximum of 935 mm in 2001.

54 storm events were extracted from this database. They correspond to those for which the simulated discharge exceeds the flooding threshold. These events differ from their maximal intensity (from 6.8 to 63.2 mm/h), duration (from 10 minutes to 8.5 hours) and total rainfall accumulation (from 7.4 to 112.8 mm). They are represented on the Intensity-Duration-Curve computed from Montsouris station located at 3 km from Châtillon. 90% of these events are characterized by a frequent return period (between 1 month and 2 years, see Figure 4). Four storms have a return period exceeding 10 years and among them, one event appears to be particularly rare with an intensity equal to 58

mm/h for a duration of one hour. In addition, the four most significant events that occurred in Trappes during the 2011-2012 campaign (and plotted in Figure 2) have been reported in Figure 4. Three of these events are characterized by a return period lesser or equal to 6 months representing very frequent rainfall. The highest is characterized by a one year return period. That means the hydrological model has been calibrated to reproduce common events and we assume it is able to represent correctly rarer events characterized by more intense precipitation.

Note that evapotranspiration data computed by the French Weather service in Villacoublay were available for the same period and has been used as PET input (same data as those used to calibrate and validate the green roof module, Section 2).

No automatic continuous stream gauge station is located on Châtillon basin. Nevertheless, a campaign was conducted from April to June in 2009 to evaluate the discharge at the outlet. The response to three rainfall events was registered. They all correspond to a total precipitation higher than 12 mm.

3-3 SWMM calibration on the current situation of the basin

Châtillon basin has been modelled in SWMM to correctly reproduce its hydrological behaviour. Its modelling representation and parameterization was provided by the Hauts-de-Seine county that use it for operational issues. The basin is split into several sub-basins (characterized by an average area of 10 ha, see Figure 3). Each sub-basin is divided in two areas (an impervious area and an infiltration area). Green roof surface is deduced from the impervious area. Each discharge component (computed for remaining impervious area, green roof area and infiltration area) is routed and summed at the sub-basin outlet. Each sub-basin contribution is then routed in the drainage network by using geometrical information of the pipes.

The Châtillon basin representation has been tested on past events. Simulations have been performed on three 2009 rainfall events for which temporal discharge observations were made. SWMM simulations (see Figure 5) are satisfactory for this kind of rainfall event with a good representation of the peak discharges and some Nash efficiencies higher than 0.85. Whereas these rainfall events are common ones –and in the absence of additional information and further validation/calibration on more severe events- it has been assumed that the model will be able to simulate the hydrological basin behaviour for more severe events (for which green roof effect will be lower).

3-4 Green roofing scenarios

To estimate the potential of green roofing, land use (IAU-IDF, 2008) and building data (IGN, 2011) have been combined. Some specific classes of the land use database have been selected assuming green roof could potentially be implemented. The hypothesis has been made that every building belonging to these classes are mainly covered by flat roofs and therefore are able to become green roofs: collecting housing, industrial and economic activities, public buildings, equipment… In each class, the roof areas have been deduced by identifying the building areas from the IGN database.

Finally, the potential of green roofing is defined as the sub-basin area that could be covered by green roof (Figures 3-b and 3-c). It is a high estimation of the real green roofing potential since it assumes that all selected buildings are effectively covered by a flat roof, without micro-structure and where green roof can technically be implemented (and is not already implemented). These potentials also represent a maximum value for which green roofing scenarios will be deduced by selecting a part of it.

In the Châtillon basin, the potential of green roofing appears to vary significantly from one sub-basin to another (Figure 3) with an average value of 1.6 ha (representing 17% of the sub-basin area). The downstream part (where individual houses are located) is characterized by a potential close to 0 ha, whereas almost all the sub-basins located upstream to the Boulevard de Vanves have a higher potential locally reaching more than 5.6 ha (corresponding to 50% of the basin area).

Different green roofing scenarios have been provided, based on the potential of green roofing computed at the sub-basin scale. They correspond, for every sub-basin, to the uniform covering of 12.5, 25, 50 and 100% of the green roofing potential with a SE3Y or a SE15Y configuration. In addition to these 8 green roofing scenarios, a scenario corresponding to the current situation without any green roof infrastructure is used to evaluate the impact of green roofing (called "Reference" for now on). In SWMM, the green roof surfaces are subtracted from the impervious areas at the sub-basin scale. The green roof module, previously integrated into SWMM, is used to compute runoff for these particular surfaces. Acting in parallel, discharges computed for every contributing surface are added to provide the total sub-basin response.

4-Methodology

To assess the hydrological impacts of green roofs on urban runoff and to identify the main variables influencing these impacts, a two-step methodology has been established.

Firstly, the SWMM model has been applied at two scales: (i) on a virtual 35 m^2 green roof similar to the experimental site, (ii) on Châtillon basin. In both cases, the model was run continuously by using the 9 previously defined green roofing scenarios on the 1993-2011 time period including the 54 rainfall events. Note that 12.5, 25, 50 and 100%

scenarios refer to the percentage of green roofing potential that is effectively covered at both scales. As the virtual roof and basin are characterized by different green roofing potential, the percentage of the total covered surfaces differs for both cases. Concerning the virtual roof, the reference configuration represents a completely impervious surface; the 100% green roofing scenario represents the current infrastructure set up in Trappes. Concerning Châtillon basin, 12.5, 25, 50 and 100% scenarios refer to the coverage of 2.5, 5, 10 and 20% of the basin area.

For operational purposes, this study has been focussed on the hydrological impacts of green roof. These impacts of green roof has been evaluated though the relative difference in terms of peak discharge (*ΔQp*) and runoff volume (*ΔV*) with the reference situation for each rainfall event (expressed in percentage):

$$\Delta Qp = \frac{(Qp\_ref - Qp\_ref)}{Qp\_ref} \times 100 \qquad \text{(Eq. 14)}$$

$$\Delta V = \frac{(V\_ref - V\_ref)}{V\_ref} \times 100 \qquad \text{(Eq. 15)}$$

Where *Qp_ref* and *V_ref* refer to peak discharge and runoff volume computed for the reference situation whereas *Qp_veg* and *V_veg* correspond to those computed for the different green roofing scenarios.

As mentioned above, virtual roof and Châtillon basin are not characterized by the same green roofing potential. Moreover, at the building scale, a roof is completely covered or not by green roof in practice. In this study, the use of progressive covering scenarios aims to compare the simulated hydrological impacts at both scales. The objective of this comparison is to study how the impacts noticed at the roof scale (that can be completely covered by green roof) can be transposed at the basin scale (that can only partially be covered) taking into account the scale effect.

Secondly, the main variables influencing the hydrological impacts of green roof at both scales (in terms of peak discharge and runoff volume reduction) have been studied. The aim of this work was to compare and eventually to link and/or predict the hydrological impacts assessed at the roof and the basin scales.

In order to analyse how the rainfall event characteristics, but also the antecedent conditions, influence the green roof impact, the relationship between several hydrometeorological variables and the maximum reduction of runoff has been studied. Note that the maximum reduction corresponds to the larger peak discharge or runoff volume reduction obtained for the different green roofing scenarios. For each of the 54 events, the computed hydrometeorological variables are: maximum 5, 30 and 60 minutes precipitation intensity (*Imax5*, *Imax30* and *Imax60*), total amount of precipitation (*Ptot*), rainfall event duration (*Durat*), antecedent precipitation accumulated during the 15 previous days (*Pant*), and estimated soil saturation at the beginning of the event (*SoilSat*, represented as the level of the SE3Y and SE15Y substrate reservoirs). Note that every variable has been statistically normalised by subtracting the mean and dividing by the standard deviation for the remainder of this study. Results of the regression on normalized data allow easier comparison of coefficients to determine relative importance in their predictive power.

The direct correlation coefficient has been calculated between each hydrometeorological variable and each hydrological impact (ΔQp and ΔV for SE3Y and SE15Y). Then a multiple stepwise regression analysis (Brown, 1998) was undertaken to identify the variables which best explain and predict the hydrological response fluctuations minimizing variables redundancy. An ($n \times p$) matrix consisting of n=54 events and $p=7$ variables was constructed. Then, ($p \times p$) correlation (*COR*) and significance (p-value) matrices were constructed using statistical software in Matlab. To assess the statistical significance, we accepted correlations with p-value <0.05 using the Student t-test. Finally, multiple stepwise regression analysis generates a linear equation that predicts a dependent variable (hydrological impacts) as a combination of several independent variables (hydrometeorological variables). A final correlation coefficient has been calculated to assess the linear combination of the selected variables and its power of predictability. This procedure has been applied on both scales (virtual roof and Châtillon basin).

In this study, a linear model has been chosen because dependent variables are expressed as relative differences and not directly as hydrological responses (discharge or volume) for which a multipower model is needed (Bois and Obled, 2003). Furthermore, it is clear independent variables are not normally distributed. But despite its limitations, multiple regression analysis represents a simple model sufficient to capture a significant fraction of the impact variability as it was done in other studies under similar conditions (Drasko, 1998; Berger and Entekhabi, 2001; Nie et al., 2011). For this reason, it will be used to analyse and compare the different hydrological impacts computed at both scales.

5- Assessment of the hydrological impact of green roof

5-1 Impact at the green roof scale

First of all, it has to be noticed that the hydrological responses of SE3Y and SE15Y configurations for the considered 54 events are quite similar for the different green roofing scenarios (It has already been noticed on the experimental site for the four main events, see Figure 2). The decrease in peak discharge due to green roofing appears to be higher for SE15Y (around 10% higher). The hydrological response for both configurations essentially differs for the low precipitation events. Most of the smallest events do not produce any response for the SE15Y configuration (for only 10 of the 40 lowest events in terms of rainfall accumulation, see Figure 6) while small runoff is generated for the SE3Y one (for 32 of the same events). Concerning the highest events, discharge tends to reach the same peak value. This has already been mentioned on the experimental green roof for the highest event of 20 mm (see Section 2-1). For this reason and for a question of readability, only the results provided with the SE15Y configuration are represented in the next figures.

As expected, the reduction of the hydrological response depends on the level of green roofing: the higher the covering, the higher the reductions in terms of peak discharge or volume (see Figure 6). As the percentage of green roof is greater than that defined at the sub-basin scale (here, the potential represents the entire area whereas at the basin scale a potential of 100% represents 20% of the total area), the hydrological impact of green roof is significant. As already mentioned, most of the rainfall events (the smallest ones in terms of total amount of precipitation) are completely retained by the 100% green roofing scenario: in this case, only 22 of the 54 rainy events produce runoff (characterized by a total amount of precipitation ranging 10.6 mm to 112.8 mm). At the roof scale, reductions of peak discharge and runoff volume are of the same order of magnitude: about 10% (ranging 6% to 12%) for a covering of 12.5% of the roof, about 20%, 40%, and 85% (ranging 13% to 25%, 37% to 50% and 10% to 100% for peak discharge) for a covering of 25%, 50% and 100% of the roof area respectively.

Surprisingly, for some particular events (N° 35, 36, 49 and 51 in Figure 6), some green roofing scenarios can produce a higher peak discharge (meaning a negative value of ΔQp) than the one generated by the entire impervious surface (or a smaller coverage scenario). An example of this situation is presented in Figure 7 (note that the other ones are similar to this event). This rainfall event that occurred on 1 December 2010 is characterized by a double rainfall peak spaced in time by 10 minutes (55.2 mm/h and 64.8 mm/h respectively). The total impervious roof responds identically with two peak discharges reaching 0.45 l/s and 0.61 l/s respectively. As expected, the crescent covering of green roof tends to reduce both peaks (12.5% and 25% green roofing scenarios generate a reduction of peak discharge of about 12% and 22%). The 50% covering implies also a significant decrease for the first peak and a less significant one for the second peak, combined with a 10-minute delay. This trend is also amplified with the 100% green roofing scenario. The first rainfall peak is completely stored in the green roof, but the second part of the event generates a peak discharge (0.61 m^3/s) higher than that produced by the total impervious roof. This is due to the concomitance of the fast response of the saturated substrate generated by the second rainfall and the slow response of the green roof produced by the first rainfall.

5-2 Impact at the basin scale

As already mentioned for the virtual roof, the difference between SE3Y and SE15Y configurations impacts are not completely negligible. Comparing to the results obtained for SE3Y, the use of SE15Y green roof implies an additional reduction of peak discharge ranging 0.3% (for 12.5% potential covering scenario) to 2.3 % (for 100% potential covering scenario). Although this difference varies from a rainfall event to another, it never reaches more than 10% for a same event (respectively 15% for the volume).

The simulated peak discharges appear to be influenced by the implementation of green roofs when significant roof surface is covered. Hydrological responses computed for the different green roofing scenarios on the study basin have been represented from smallest to largest in Figure 8. Although the impact of green roof varies from one storm event to another, the covering of only 12.5% on the green roofing potential implies a small reduction of the peak discharge (average value of 4.7%, from a minimum of 0% to a maximum of 5.5%). This reduction of peak discharge slightly increases with the covering of 25% (the reduction ranges from 3.5% to 10.2% with an average value of 9%). For both low green roofing scenarios, the impact on runoff volume is quite negligible with an average decrease of 6.6% in the best case (25% covering scenario).

High green roofing scenarios (covering of 50 or 100% of the potential) have more valuable consequences in terms of runoff reduction. The 50% scenario leads to an average peak discharge decrease of about 18.6% (from a minimum of 9.3% to a maximum of 23.7% depending on the event). The impact of the 100% scenario looks proportional with an average *Qp* reduction of 35.6% (between 17.4% and 38.7%). The runoff volume is also significantly reduced with an average value of 25.2% for the best case, and a stronger fluctuation from a storm event to another (from 14.4% to 53.9%). Indeed, the hydrological benefit seems to be directly related to the storm event. From an operational point of view, green roofing of a significant part of the buildings' roofs implies the reduction of the flooding risk: 14 rainfall events (on 54) now have a peak discharge lower than the flooding threshold of 4.7 m^3/s for the 50% scenario, and 26 events for the 100% scenario respectively.

The situation presented in the previous section, where peak discharge is increased by the use of green roof, does not occur at the basin scale. It is explained in part by the specific configuration of the case study, especially the spatial repartition of the impervious and green roof surfaces and the attenuation effect of the sewer network.

5-3 Correspondence between virtual roof and basin impacts

When comparing results obtained for virtual roof and Châtillon basin, green roof impacts (on peak discharge or runoff volume) appear to not perfectly match from one rainfall event to another. The sensitivity to green roof implementation and the magnitude of these impacts is clearly different because the average green roof potential is 20% on the study basin while it represents the entire area on the virtual roof. For this reason, in many situations, runoff is completely avoided on the virtual roof, whereas it is only reduced (at most 40%) on the basin.

Nevertheless, both studied surfaces follow more or less the same trend, and differences seem to be devoted to the specific configuration of the sewer network and layout between impervious and green roof surfaces. Although green roof can reduce the hydrological impact of stormwater, these consequences are conditioned by the intrinsic properties of the studied basin. The main difference occurred for two severe rainfall events characterized by a total accumulation of 63.8 and 112.8 mm for a duration of 65 and 515 minutes respectively (Events No 50 and 52, see also Figure 4) for which the 10-year return period was exceeded. In these situations, the impact noticed at the roof scale is significantly attenuated at the basin scale. The influence of remaining impervious areas and the saturation of the substrate seem to cancel runoff reduction abilities of green roof.

At both scales (roof and basin), hydrological impact of green roof seems also to be related to the specific characteristics of the rainfall event. Regarding Figures 6 and 8, the relative reduction of peak discharge seems to be higher for the smallest events in terms of rainfall amount. This observation that has already been mentioned in previous studies (Carso*n et al*., 2013; Fassman-Bec*k et al*., 2013) and will be studied in detail in the following.

6-Condition of urban runoff reduction

Simple correlation and multiple stepwise regression analysis have been undertaken to identify which variables (*Imax5*, *Imax30, Imax60*, *Ptot*, *Durat*, *Pant*, *SoilSat*,) can explain and can predict hydrological response fluctuations (ΔQp and ΔV) minimizing variables redundancy.

6-1 At the virtual roof scale

Regarding the single correlation coefficients (Table 2), precipitation seems to be an important factor influencing the hydrological response. Despite the 5-minute time period being close to the response time of the virtual roof (assessed from observation on Trappes' roof characterized by a time to peak reaching 3 to 6 minutes), the accumulations on higher time periods (one hour or on total event duration) seem more predominant. As mentioned in recent studies (Carso*n et al*., 2013; Fassman-Bec*k et al*., 2013), the higher the precipitation, the lower the hydrological impact (in terms of reduction of peak discharge and runoff volume). These durations are usually close to the time separating the end of rainfall and the end of runoff (observed as being higher than 30 minutes).

Whatever the green roof configuration, the duration of the event and the antecedent precipitation are weakly correlated with hydrological responses. Antecedent conditions seem to be better represented by the substrate saturation at the beginning of the event. The correlation with this variable is also higher for the thicker substrate (around 0.70) meaning the SE3Y configuration response does not depend much on initial conditions. As it has a smaller water retention capacity, substrate generally has time to dry between two events and it is rapidly saturated for the most severe events.

The multiple stepwise regression analysis selects almost the same hydrometeorological variables to optimize the multilinear correlations (see Table 2): total rainfall accumulation and estimated soil saturation at the beginning of the event for peak discharge reduction. An additional variable (Imax60) influences runoff volume reduction. As *Imax5*, *Imax30*, *Imax60* and *Ptot* are strongly correlated, only one or two variables among them are considered as statistically significant at the <.05 level. The selection of *Imax60* and *Ptot* for volume reduction can be interpreted as follows: the 1-hour accumulation close to the concentration time of the roof. If the rainfall event continues after this duration, most of the precipitation becomes directly runoff, influencing the total volume.

The final correlation computed by using the selected variables is quite good for both configurations and both hydrological impacts (from 0.68 to 0.90). The scatter plots comparing observed and simulated hydrological impacts are presented in Figure 9. Most of the points are located close to the symmetric line. Two main reasons can be proposed in order to explain the different outliers and the difficulty for the multilinear relationship to reproduce some specific situations. First, the threshold effect is noticed for several events for which no runoff is produced by the SE15Y configuration (ΔQp and ΔV are equal to 100%). Second, singular behaviours can occur as those produced by concomitance situations (as shown in Section 4-2): in these cases, two consecutive peaks of rain produce a peak discharge reduction not significant as expected, and can sometimes amplify the reference situation.

Similar regression analysis was performed by Stovin *et al.* (2012) for similar results. They tried to link several hydrometeorological variables to the direct hydrological consequence of green roof and not the relative differences as in this study. Total rainfall accumulation appeared to be linked to runoff depth and percentage of retention (correlation coefficients of 0.72 and 0.33 respectively). The influence of antecedent dry weather period seemed to be more complex and the combination of several variables showed it was not to possible to predict retention depth for a particular hydrometeorological situation.

6-2 At the Châtillon basin scale

At the basin scale, the results of correlation are quite similar to those obtained at the virtual roof scale. As expected, precipitation is strongly correlated to the peak discharge reduction (the higher the total precipitation, the lower the reduction), while runoff volume reduction is hardly explained by the independent variables. Only the antecedent condition in terms of estimated soil saturation seems to influence the volumetric response and is considered as statistically significant at the p-value<0.05 level.

The multiple stepwise regression analysis selects almost the same hydrometeorological variables as at the roof scale (see Table 2): total rainfall accumulation and estimated soil saturation at the beginning of the event. Note that despite their strong correlation, *Imax30*, *Imax60* and *Ptot* are selected to explain the peak discharge reduction for SE3Y configuration. They correspond to different scales of the basin response. Nevertheless, these results from multiple stepwise regressions should be interpreted with some caution because of: (i) the limited sample data (54 events for 7 independent variables), (ii) the clearly non-normal distribution of these variables, and (iii) few outliers due to singular behavior.

The comparison between simulated and stepwise computed hydrological impacts is also well represented on the scatter plots (Figure 10). The peak discharge impacts are well depicted around the symmetric line and only a few events are located far from the median values. They correspond to the two main events characterized by a total rainfall accumulation of 112.8 mm and 63.8 mm. It appears the basin is able to smooth a large majority of the events and only react to the extreme ones.

The distribution of total runoff volume is more erratic with a wide dispersion around the symmetric line. Estimated soil saturation at the beginning of the event is the only selected variable explaining ΔV fluctuations for the SE15Y configuration. This variable is characterized by low fluctuations (ranging from 12% to 35% for an average value of 17%). As a consequence, many volume reductions are estimated by a constant simulated value, representing an unsaturated substrate at the beginning of the event.

6.3 Is roof scale impacts a good indicator to predict basin scale impacts?

Obviously, green roofing impacts are easier to observe at roof scale than at basin scale. In addition, previous results have shown that the main hydrometeorological factors influencing hydrological impacts are quite similar at both scales: initial soil moisture condition and intensity or accumulated precipitation. In order to appreciate how estimated results at roof scale may help to predict impact at the basin scale, the hydrological impacts noticed at the basin scale have also been compared to those computed at the roof scale by using the multi-linear regression (Figure 11). Although correlation coefficients are always lower than those obtained by using the multi-linear regression calibrated at basin scale, they provide satisfactory results. It appears correlation coefficients are higher for peak discharge concerning SE3Y (0.84) and for runoff volume concerning SE15Y (0.71) respectively. This is due to the common selected hydrometeorological variables (characterized by high correlation) shared by both case studies: *Ptot* and *SoilSat* for ΔQp and *SoilSat* for ΔV. These results show that impacts estimated at roof scale can globally approximate those expected at basin scale for a large set of rainfall events by using a reduction coefficient. This approximation can appear quite rough but can be useful to have an idea of the consequence of green roof at the basin scale.

7-Discussion

These encouraging results provided by a modelling approach are based on a number of implicit hypotheses and limitations that can be discussed:

(1) The SWMM representation of green roof at the sub-basin scale. First, the estimation of the green roofing potential may look optimistic. The methodology used probably overestimates the real potential. It is assumed that all buildings belonging to the selected land use categories can effectively be covered by green roof, meaning that they have flat roofs, without micro-structure and for which the implementation of green roof is technically possible (and already done). The consideration of only a fraction of this potential seems to be more realistic. For this reason, these results illustrate the potential of such structures and encourage the implementation of green roofs for future rehabilitation and developing

projects. Second, green roof areas are considered as a unique entity at the sub-basin scale (mean area of 10 ha), without taking into account the spatial distribution of the green roof covered buildings. This may impact the dynamic of the response by using the Manning-Strickler equation on a virtual area representing the sum of the different covered roofs. For this reason, we assume such a representation is adapted to assess the hydrological impact of green roof at the basin scale but surely not at the sub-basin one.

(2) The short time period for the calibration of the hydrological model. The model parameters have been adjusted by using 1-year observation data during which no severe event was observed (the maximum exceeded return period is equal to 1 year). That means the model has been calibrated on common events, and we assume it is able to correctly represent rarer events characterized by more intense precipitation. This could explain why hydrological impacts computed for extreme events are often located far from the regression line (linking SWMM simulated and stepwise computed hydrological impacts). For this reason, the observation of experimental green roofs has to continue in order to capture more significant storm events. These additional data will be used to improve and/or validate the model in the future. However, the use of current data allows us to conclude that the implementation of green roof can be useful to limit the consequences of common storm events on sewage network. Moreover, evapotranspiration has appeared as a key factor influencing initial substrate saturation during wet periods. The improvement of its estimation could improve model simulations.

(3) The specific configuration of the studied basin. The presented results have been computed for a particular urban basin belonging to the Hauts-de-Seine county.

For this reason, the figures obtained in terms of flooding reduction can not be generalized and transferred to other locations. Indeed, they depend on the basin configuration, especially on green roofing potential (with the diffusion more or less significant of flat roof), the combination of impervious and green roofing surfaces, but also on the basin geometry and the sewage network arrangement. For these reasons, it is quite possible that some concomitance situations occur as noticed at the roof scale in Section 4-2. The superposition of responses from an impervious area and a green roof area to a complex rainfall event (composed by several rainfall peaks for example) can generate a peak discharge higher than that produced by the current (impervious) situation.

8-Conclusions

Based on experimental green roof observations, a conceptual hydrological model has been developed and calibrated to reproduce the hydrological behaviour of two different types of green roof differentiated by their substrate depth. On the other side, several green roofing scenarios have been produced for a small urban basin, ranging from the current situation (no green roof is implemented) to a maximum roof area that can be covered by green roof. Integrated into the stormwater management model SWMM, the conceptual hydrological model has been applied on a large time series at the basin scale to assess its impact in terms of urban water management. For comparison, the same procedure has also been applied at the roof scale. Finally, a complementary analysis has been conducted to study which hydrometeorological variables can influence the magnitude of these hydrological impacts at both scales.

Whether at the scale of roof or basin, green roof appears to significantly impact urban runoff in terms of peak discharge and volume. At the roof scale, the obtained results for a complete green roof covering (reduction close to 90% for peak discharge and runoff volume) are similar to those provided by experimental studies (Voyde *et al.*, 2010 ; Palla *et al.*, 2011 ; Stovin *et al.*, 2012). At the basin scale of our case study, results are less pronounced because they depend on the green roofing potential of each sub-basin, which usually represents around 20% of the sub-basin area (2.37 km^2). The reduction of the hydrological response (peak and volume runoff) can reach almost 20% when half of the potential is covered and more than 35% for the entire area. It seems to be enough to avoid some flooding issues in several cases as demonstrated on our case study: for 14 of the 54 considered rainfall events, modified peak discharge are then lower than the flooding threshold with the 50% green roofing scenario.

It has also been noticed that the response of the two SE3Y and SE15Y green roof configurations (substrate depth of 3 and 15cm) for the 54 studied events are quite similar. The hydrological responses of both configurations essentially differ for the low precipitation events, for which the thicker substrate produces less runoff. For the highest ones, both peak discharges and runoff volumes are of the same order. This has already been observed on the experimental green roof for the more intense events, but also in some previous studies. Voyde *et al.* (2010), for example, mentioned that an increase in substrate depth from 50 mm to 70 mm did not provide a measurable increase in hydrological performance.

By comparing several hydrometeorological variables relative to the rainfall events with the hydrological impacts of green roof (at roof and basin scale), it appears that precipitation –generally accumulated during the whole event- and initial substrate saturation are both influencing variables: the higher the precipitation, the more saturated the substrate, and the lower the reduction in terms of stormwater. The use of green roof seems to be helpful to mitigate the effects of a rainfall event characterized by a return period lower than 10 years. For the more severe events, the impact of green roof is marginal and can not be used to solve operational issues.

At both scales (roof and basin), it appears difficult to forecast the hydrological impacts of green roof only by considering hydrometeorological variables. Multilinear relationships approximate responses (in terms of peak discharge and runoff volume) to storm water, but they fail in reproducing them correctly for a large kind of rainfall event and antecedent condition configurations. They need a more physical tool (a hydrological model) to estimate the consequences of the involved non-linear processes. Moreover, the basin response seems to be deeply influenced by its own configuration. Nevertheless, in a first approximation, the multi-linear relationship adjusted for the roof can provide correct estimation at the basin scale.

Despite some limitations mentioned in the previous section, this study supports the large scale implementation of green roofs to locally reduce overflows in the drainage network. In addition to possible thermal and environmental benefits, green roof can be valuable from an urban water management point of view. As already mentioned in other studies (Carter and Jackson, 2007), green roofs alone cannot solely be relied upon to provide complete stormwater management at the watershed scale. Combined with other stormwater source controls or/and retention infrastructures, green roof could contribute to significant reductions of the quantity of water flowing into the sewage network during storm events. A combination of source control management strategies and water reuse techniques are more cost effective than their traditional centralized counterpart (Coombes *et al.*, 2002). As a result, this kind of study could be used by policy makers and water management authorities to promote the dissemination of green roof in the future.

Acknowledgments

This work has been supported by the French C2D2 framework programme through the TVGEP project. The authors would like to thank the Water Direction of the Haut-de-Seine county, especially Pascal Jouve, Christian Roux and Christophe Lehoucq, for providing geographical and hydrometeorological data and expertise.

Bibliography

Banting, D., Doshi, H., Li, J. and Missios, P., 2005. Report on the Benefits and Costs of Green Roof Technology for the City of Toronto.

Bengtsson, L., Grahn, L. and Olsson, J., 2005. Hydrological function of a thin extensive green roof in southern Sweden. Nordic Hydrology 36: 259-268

Berger, K.P. and Entekhabi, D., 2001. Basin hydrologic response relations to distributed physiographic descriptors and climate. Journal of Hydrology, 247(3-4): 169-182.

Berndtsson, J.C., 2010. Green roof performance towards management of runoff water quantity and quality: A review. Ecological Engineering, 36(4): 351-360.

Berthier, E., Ramier, D. and de Gouvello, B., 2011. Simulation of green roof hydrological behavior with a reservoir model. In: International Water Association (Editor), 12th International Conference on Urban Drainage, Porto Alegre (Brazil), pp. 8.

Bois, P. and Obled, C., 2003. Introduction au traitement de données en Hydrologie, L'Edition du Millénaire, Institut National Polytechnique de Grenoble.

Brown, C.E., 1998. Applied multivariate statistics in Geohydrology and related sciences. Springer-Verlag, Berlin.

Carson, T.B., Marasco, D.E., Culligan, P.J. and McGillis, W.R., 2013. Hydrological performance of extensive green roofs in New York City: observations and multi-year modeling ofÂ three full-scale systems. Environmental Research Letters, 8(2): 24-36.

Carter, T. and Jackson, C.R., 2007. Vegetated roofs for stormwater management at multiple spatial scales. Landscape and Urban Planning, 80(1-2): 84-94.

Carter, T.L. and Rasmussen, T.C., 2006. Hydrologic Behavior of Vegetated Roofs. Journal of the American Water Resources Association, 42(5): 1261-1274.

Coombes, P.J., Kuczera, G., Kalma, J.D. and Argue, J.R., 2002. An evaluation of the benefits of source control measures at the regional scale. Urban Water, 4(4): 307-320.

Delleur, J., 2003. The Evolution of Urban Hydrology: Past, Present, and Future. Journal of Hydraulic Engineering, 129(8): 563-573.

Denardo, J.C., Jarett, A.R., Manbeck, H.B., Beattie, D.J. and Berghage, R.D., 2005.

Stormwater mitigation and surface temperature reduction by green roofs. Transactions of the ASAE 48(4): 1491-1496.

Drasko, F., 1998. Application example of neural networks for time series analysis:: Rainfallâ€“runoff modeling. Signal Processing, 64(3): 383-396.

Dunnett, N. and Kingsbury, N., 2004. Planting Green Roofs and Living Walls Timber Press, Portland, 336 pp.

Dunnett, N., Nagase, A., Booth, R. and Grime, P., 2008. Influence of vegetation composition on runoff in two simulated green roof experiments. Urban Ecosystems, 11(4): 385-398.

Egodawatta, P., Thomas, E. and Goonetilleke, A., 2009. Understanding the physical processes of pollutant build-up and wash-off on roof surfaces. Science of The Total Environment, 407(6): 1834-1841.

Fassman-Beck, E., Voyde, E., Simcock, R. and Hong, Y.S., 2013. 4 Living roofs in 3 locations: Does configuration affect runoff mitigation? Journal of Hydrology, 490: 11-20.

Getter, K.L., Rowe, D.B. and Andresen, J.A., 2007. Quantifying the effect of slope on extensive green roof stormwater retention. Ecological Engineering, 31(4): 225-231.

Gregoire, B.G. and Clausen, J.C., 2011. Effect of a modular extensive green roof on stormwater runoff and water quality. Ecological Engineering, 37(6): 963-969.

Gromaire, M.-C., D., R., Seidl, M., Berthier, E., Saad, M. and de Gouvello, B., 2013. Incidence of extensive green roof structures on the quantity and the quality of runoff waters, NOVATECH, Lyon (France), 10 pp.

Gromaire, M.C., Robert-Sainte, P., Bressy, A., Saad, M., De Gouvello, B. and Chebbo, G., 2011. Zn and Pb emissions from roofing materials--modelling and mass balance attempt at the scale of a small urban catchment. Water Science and Technology, 63(11): 2590-2597.

Hilten, R.N., Lawrence, T.M. and Tollner, E.W., 2008. Modeling stormwater runoff from green roofs with HYDRUS-1D. Journal of Hydrology, 358(3-4): 288-293.

IAU-IDF, 2008. Base de connaissance sur le Mode d'Occupation du Sol (MOS).

IGN, 2011. BD TOPO® Descriptif de contenu.

Lassalle, F., 2012. Panorama technique, historique et géographique, Paris (France). 20th November 2012

Mentens, J., Raes, D. and Hermy, M., 2006. Green roofs as a tool for solving the rainwater runoff problem in the urbanized 21st century? Landscape and Urban Planning, 77(3): 217-226.

Mockus, V., 1957. Use of storm and watersheds characteristics in synthetic hydrograph analysis and application. U.S. Dept. of Agriculture, Washington (USA).

Monterusso, M.A., Rowe, D.B., Rugh, C.L. and Russell, D.K., 2004. Runoff water quantity and quality from green roof systems. Acta Horticulturae (ISHS) 639: 369-376.

Nash, J.E. and Sutcliffe, J.V., 1970. River flow forecasting through conceptual models part I - A discussion of principles. Journal of Hydrology, 10(3): 282-290.

Nature, E., 2003. Green Roofs: Their Existing Status and Potential for Conserving Biodiversity in Urban Areas, Peterborough.

Nie, W., Yuan, Y., Kepner, W., Nash, M.S., Jackson, M. and Erickson, C., 2011. Assessing impacts of Landuse and Landcover changes on hydrology for the upper San Pedro watershed. Journal of Hydrology, 407(1-4): 105-114.

Palla, A., Berretta, C., Lanza, L.G. and La Barbera, P., 2008. Modelling storm control operated by green roofs at the urban catchment scale 11th International

Conference on Urban Drainage, Edinburgh (Scotland).
Palla, A., Gnecco, I. and Lanza, L.G., 2009. Unsaturated 2D modelling of subsurface water flow in the coarse-grained porous matrix of a green roof. Journal of Hydrology, 379(1-2): 193-204.
Palla, A. Sansalone, J.J., Gnecco, I. and Lanza, L.G., 2011. Storm water infiltration in a monitored green roof for hydrologic restoration. Water Science and Technology, 64(3), 766-773
Petrucci, G., Rioust, E., Deroubaix, J.-F. and Tassin, B., 2012. Do stormwater source control policies deliver the right hydrologic outcomes? Journal of Hydrology.
Rossman, L.A., 2004. Storm water management model User's manual version 5.0, Water Supply and Water Resources Division, National Risk Management Research Laboratory, Cincinnati (USA).
Santamouris, M., 2012. Cooling the cities - A review of reflective and green roof mitigation technologies to fight heat island and improve comfort in urban environments. Solar Energy(In press).
Simmons, M.T., Gardiner, B., Windhager, S. and Tinsley, J., 2008. Green roofs are not created equal: the hydrologic and thermal performance of six different extensive green roofs and reflective and non-reflective roofs in a sub-tropical climate. Urban ecosystems 11(4): 339-348.
Šimůnek, J., Vogel, T. and Van Genuchten, M.T., 1994. The SWMS_2D code for simulating water flow and solute transport in two-dimensional variably saturated media, Version 1.21, Research Report No. 132, , Riverside, California (USA).
Šimůnek, J., van Genuchten, M.T. and Šejna, M., 2008. Development and applications of the HYDRUS and STANMOD software packages, and related codes. Vadose Zone Journal, 7(2): 587-600.
Stovin, V., Vesuviano, G. and Kasmin, H., 2012. The hydrological performance of a green roof test bed under UK climatic conditions. Journal of Hydrology, 414-415(0): 148-161.
Takebayashi, H. and Moriyama, M., 2007. Surface heat budget on green roof and high reflection roof for mitigation of urban heat island. Building and Environment, 42(8): 2971-2979.
Urbonas, B. and Jones, J.E., 2002. Summary of Emergent Urban Stormwater Themes, Linking Stormwater BMP Designs and Performance to Receiving Water Impact Mitigation. American Society of Civil Engineers, pp. 1-8.
Villarreal, E., 2007. Runoff detention effect of a sedum green-roof. Nordic hydrology, 38(1): 99-105.
Villarreal, E.L. and Bengtsson, L., 2005. Response of a Sedum green-roof to individual rain events. Ecological Engineering, 25(1): 1-7.
Voyde, E., Fassman, E. and Simcock, R., 2010. Hydrology of an extensive living roof under sub-tropical climate conditions in Auckland, New Zealand. Journal of Hydrology, 394(3-4): 384-395.

Figure captions

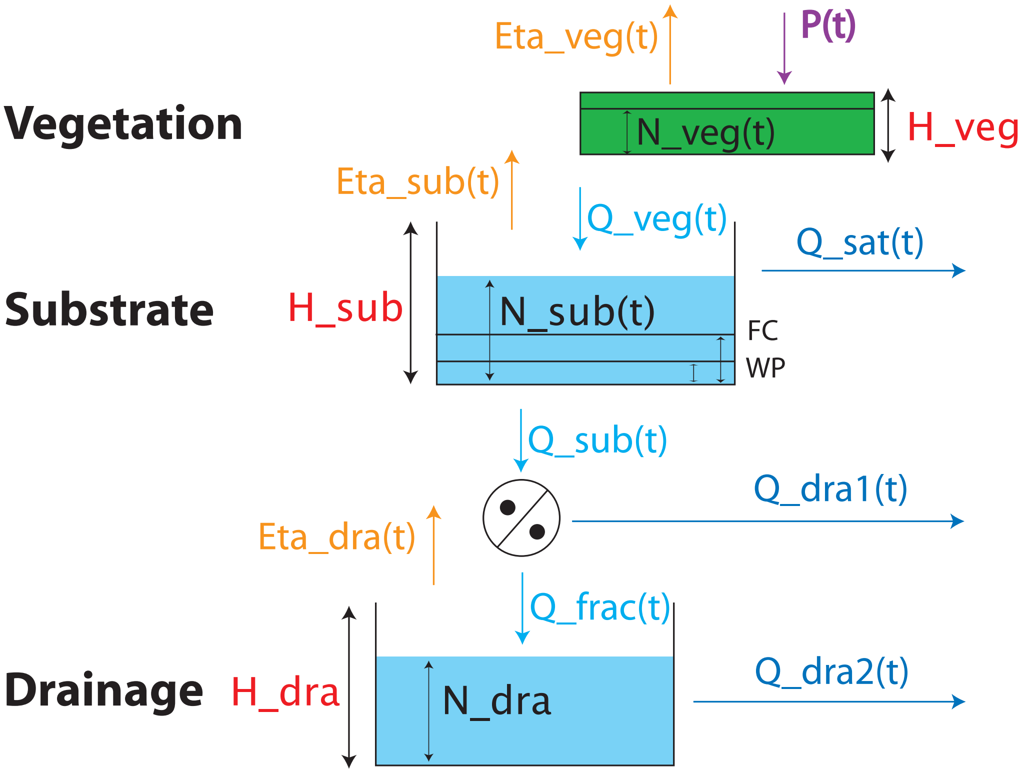

Figure 1: Reservoir model developed in SWMM (notations are explained in the text)

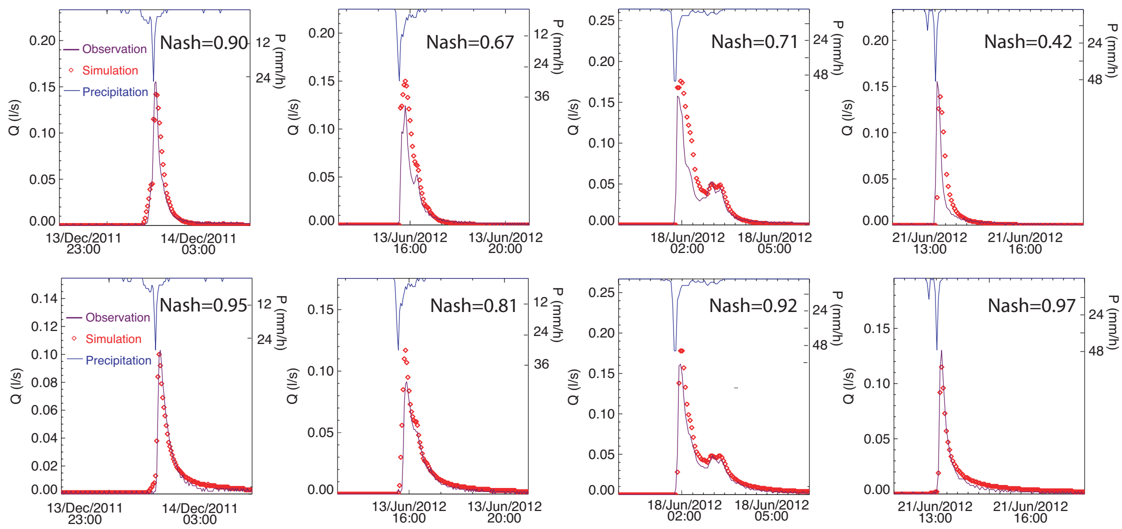

Figure 2: Comparison between observed and simulated discharges computed at the roof scale. Results obtained for the four most severe events of the study period (June 2011-

August 2012) are presented for SE3Y (top) and SE15Y (bottom) green roof configurations.

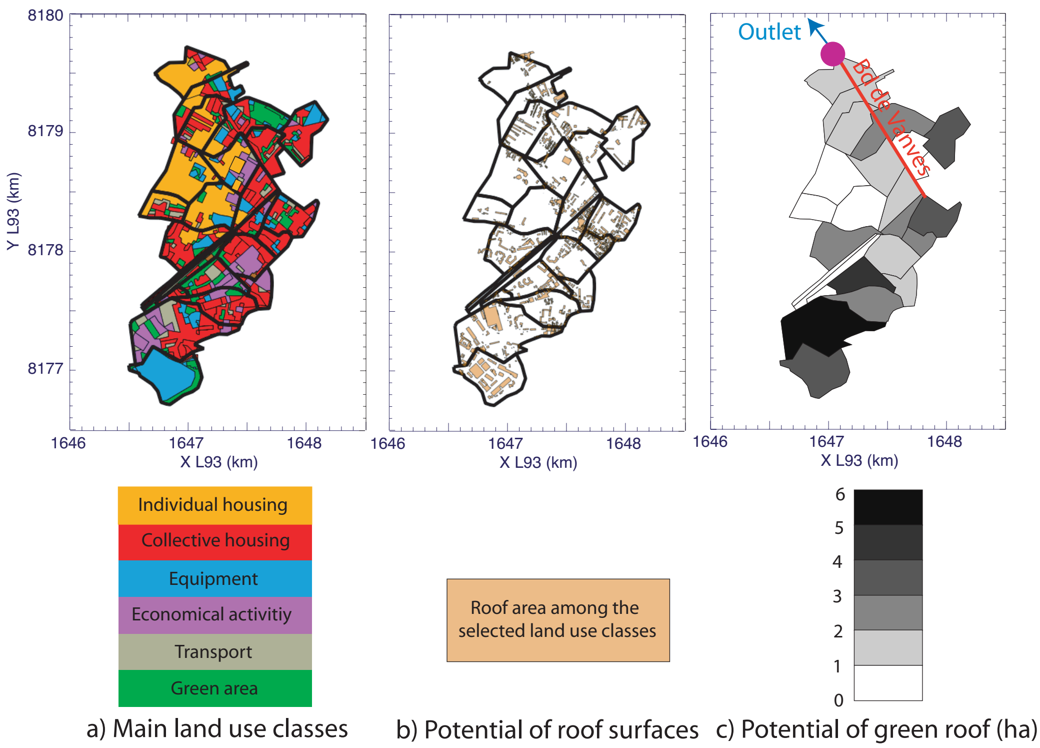

Figure 3. Châtillon basin disaggregated into 25 sub-basins for SWMM modelling: a) land use distribution, b) potential roof surfaces distribution, c) green roofing potential distribution

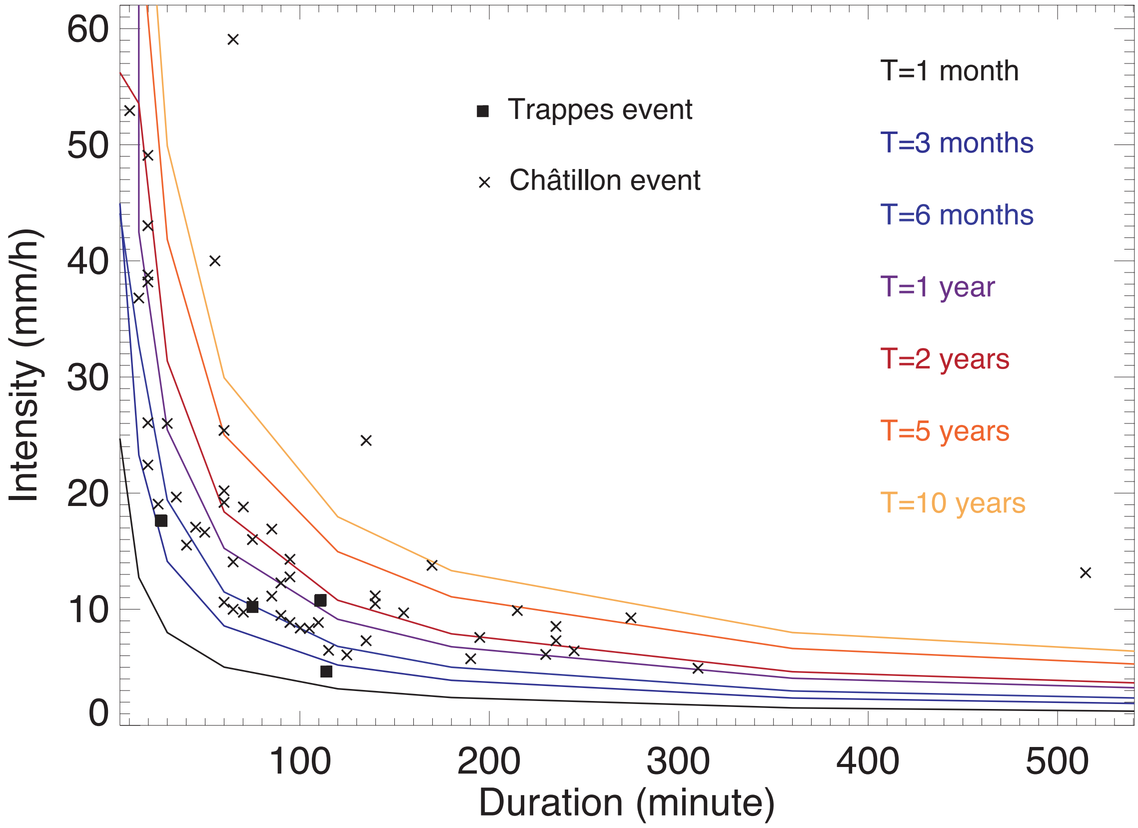

Figure 4. Characterization of the studied rainfall events in terms of duration and intensity, IDF curves from Montsouris (Paris, France) are indicated. The 54 events computed from Hauts-de-Seine database on the 1993-2011 period are represented by crosses and those computed from the experimental green roof in Trappes on the 2011-12 period are represented by squares.

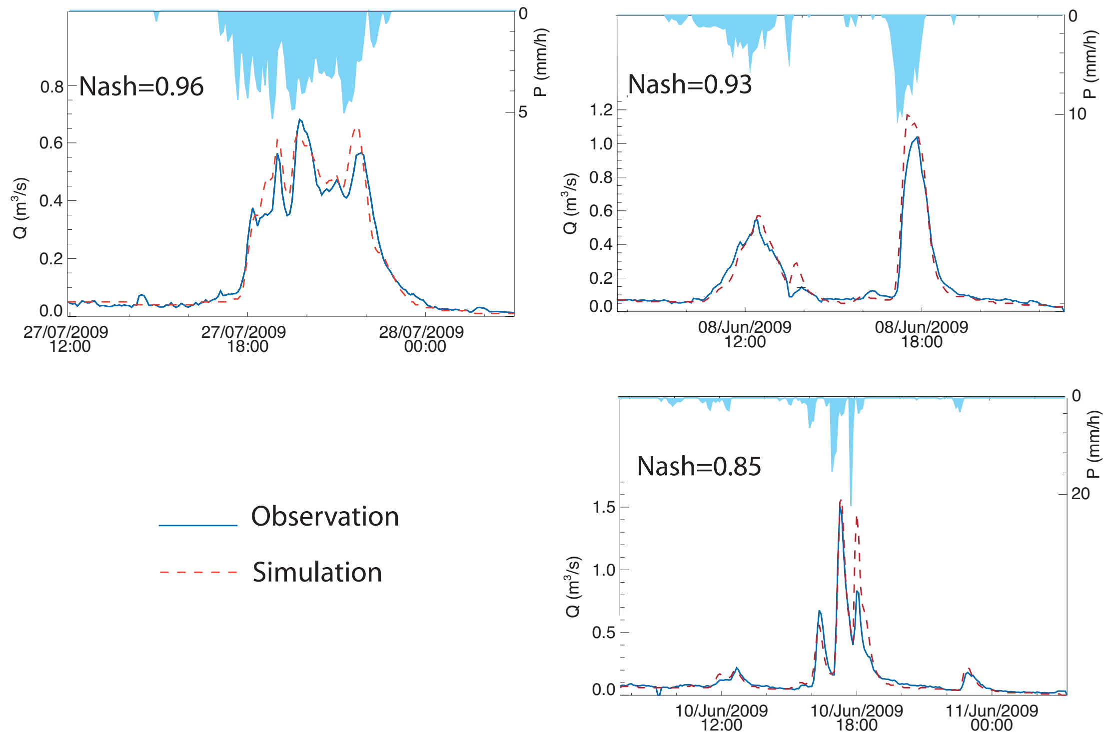

Figure 5: Comparison between observed and simulated (with SWMM) discharge computed at the Châtillon basin scale. Simulations were performed on three 2009 rainfall events for which temporal discharge observations were available.

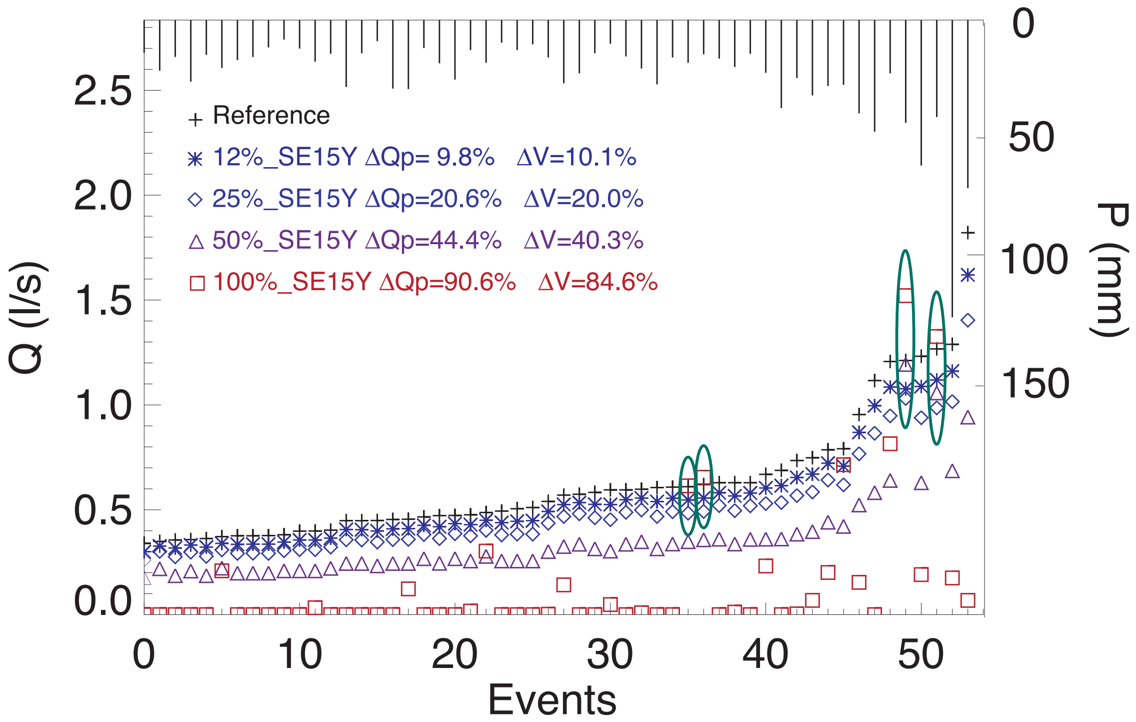

Figure 6. Impact of the green roofing scenarios on the 35 m^2 virtual roof: peak discharge is represented for the 54 rainfall events (ordered by increasing value of *Qp*), the average reduction in peak discharge (*ΔQp*) and runoff volume (*ΔV*) are indicated for the four green roofing SE15Y scenarios. The total amount of precipitation is also represented for every event (bars on inverse axes) and the particular events for which the implementation of green roof produces higher peak discharge are surrounded.

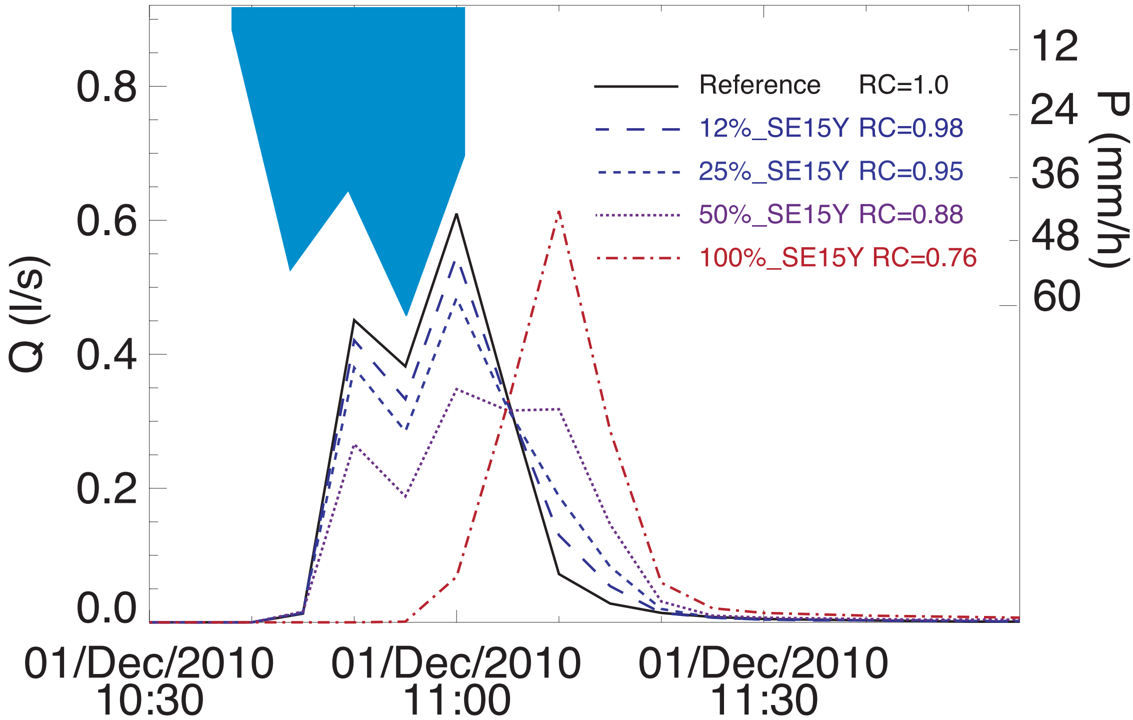

1038

1039 Figure 7. Hydrological response of the virtual roof for different greening scenarios on
1040 the 1st December 2010 rainfall event. Precipitation is represented, in blue, on the
1041 inverse axes. Runoff coefficients (RC) are also indicated.

1042

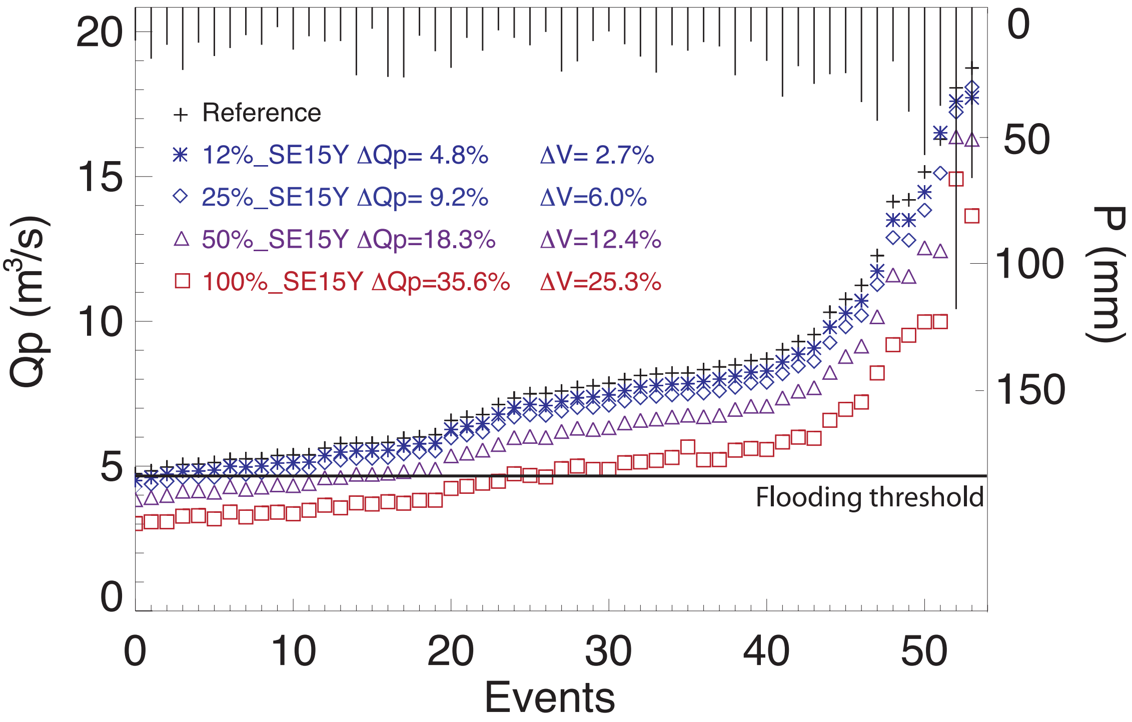

Figure 8. Impact of the green roofing scenarios on the basin: peak discharge is represented for the 54 rainfall events (ordered by increasing value of *Qp*): the average reduction in peak discharge (*ΔQp*) and runoff volume (*ΔV*) are indicated for the four SE15Y scenarios. The total amount of precipitation is also represented for every event (bars on inverse axes).

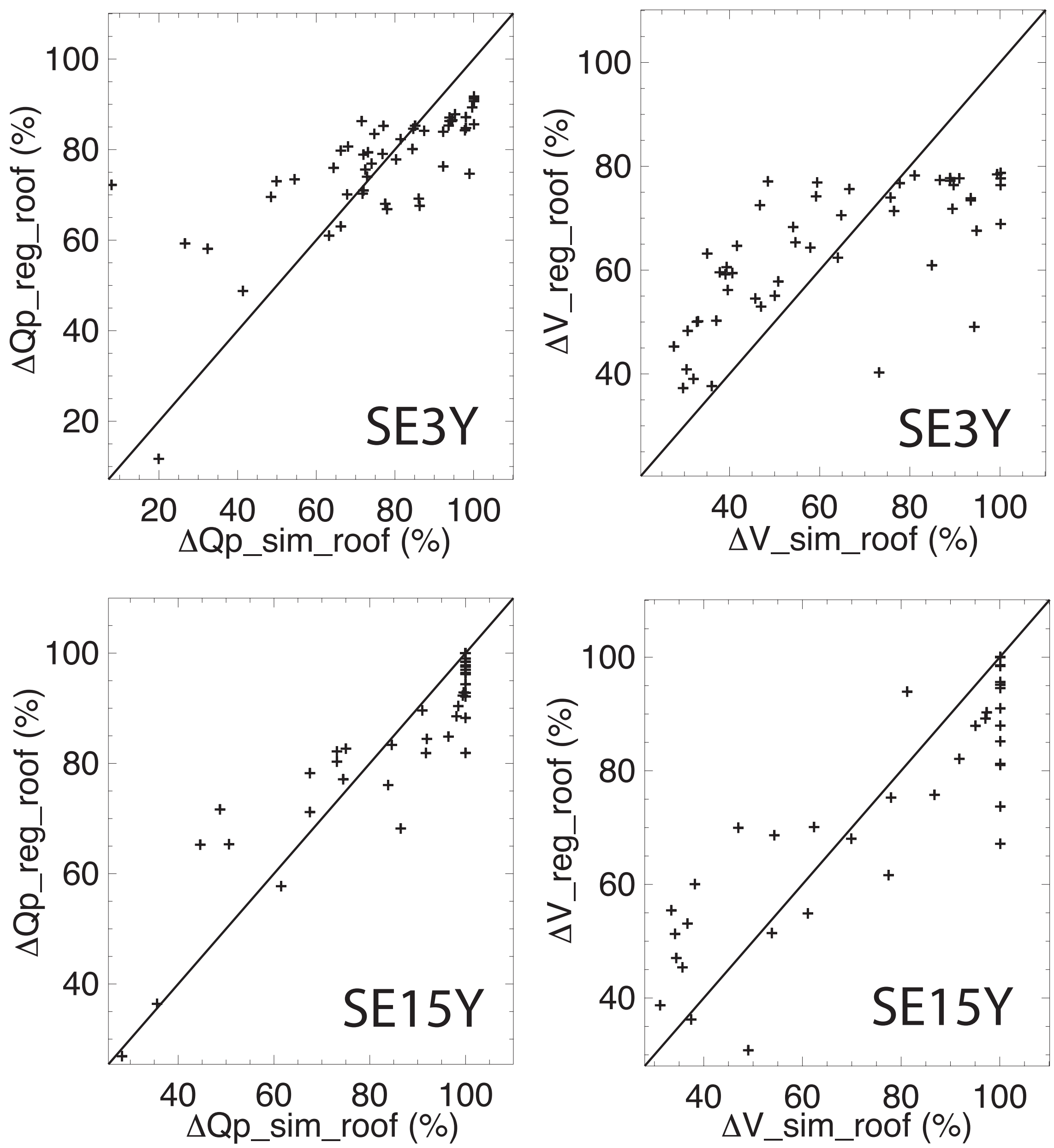

Figure 9. Comparison between SWMM simulated (sim) and stepwise computed (reg) hydrological impacts (*ΔQp* and *ΔV*) at the virtual roof scale for SE3Y and SE15Y configurations and the 100% green roofing scenario (the solid line corresponds to the x=y symmetric equation).

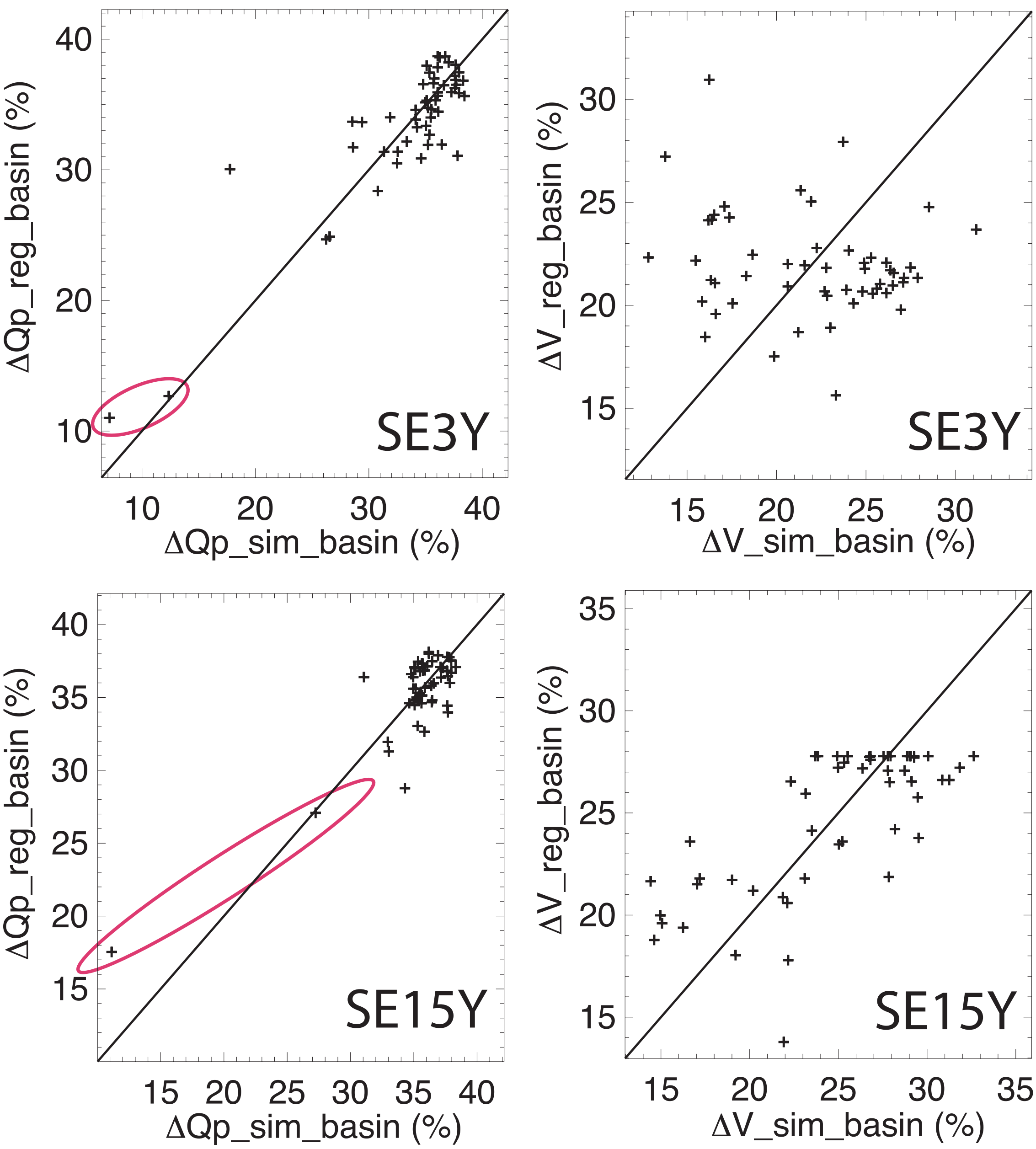

Figure 10. Comparison between SWMM simulated (sim) and stepwise computed (reg) hydrological impact (*ΔQp* and *ΔV*) at the basin scale for SE3Y and SE15Y configurations and the 100% green roofing scenario (the solid line corresponds to the x=y symmetric equation). The two more intense events are surrounded.

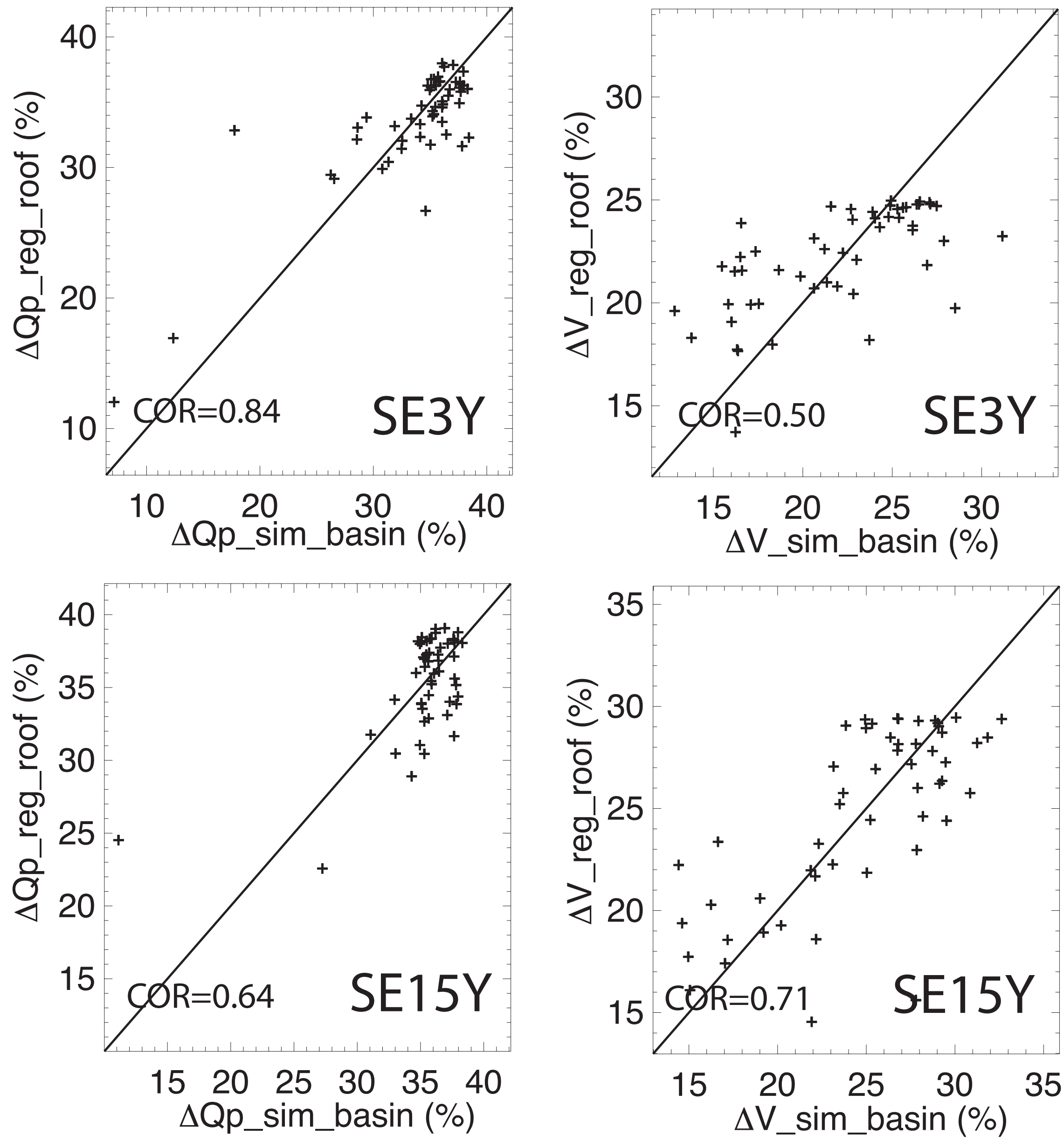

Figure 11. Comparison between SWMM simulated (sim) at the basin scale and stepwise computed at the roof scale (reg) hydrological impact (ΔQp and ΔV) for SE3Y and SE15Y configurations. The 100% green roofing scenario (the solid line corresponds to the x=y symmetric equation).

Table captions

Table 1. Calibrated parameters values for both SE3Y and SE15Y. Physical values provided by green roof supplier are indicated for comparison.

		f_sub	*FC*	*Ksat* (mm/h)	*R*
SE3Y	Physical	0.4	0.4	1158	~ 0.4
	Calibrated	*0.4*	0.39	104.7	0.51
SE15Y	Physical	0.4	0.4	1158	~ 0.4
	Calibrated	*0.4*	0.21	2.0	0.65

Table 2. Correlation between the hydrological impact and several hydrometeorological variables for virtual roof (top) and the Châtillon basin (bottom): The variables selected by the stepwise procedure are marked in bold. The last column represents the final correlation coefficient computed by using these selected variables.

At the roof scale								
	Imax5	Imax30	Imax60	Ptot	Durat.	Pant.	SoilSat	COR
ΔQ_SE3Y	-0.47	-0.69	-0.67	**-0.71**	-0.44	-0.24	**-0.36**	0.75
ΔV_SE3Y	-0.38	-0.49	**-0.48**	**-0.54**	-0.45	-0.27	**-0.44**	0.68
ΔQ_SE15Y	-0.50	-0.71	-0.69	**-0.69**	-0.40	-0.38	**-0.68**	0.90
ΔV_SE15Y	-0.50	-0.46	**-0.46**	**-0.50**	-0.34	-0.44	**-0.76**	0.89
At the basin scale								
	Imax5	Imax30	Imax60	Ptot	Durat.	Pant.	SoilSat	COR
ΔQ_SE3Y	-0.62	**-0.84**	**-0.79**	**-0.78**	-0.40	-0.14	**-0.31**	0.88
ΔV_SE3Y	-0.23	-0.25	-0.22	-0.27	**-0.26**	-0.27	**-0.42**	0.52
ΔQ_SE15Y	-0.50	-0.76	-0.81	**-0.86**	-0.54	-0.06	-0.12	0.86
ΔV_SE15Y	-0.22	-0.12	-0.10	-0.13	-0.14	-0.45	**-0.72**	0.72